frontiers in Materials

ORIGINAL RESEARCH
published: 27 April 2021
doi: 10.3389/fmats.2021.659655

Robust Silica–Polyimide Aerogel Blanket for Water-Proof and Flame-Retardant Self-Floating Artificial Island

Riyong Liu[1,2], Jin Wang[2], Jianhe Liao[1]* and Xuetong Zhang[2,3]**

[1] School of Materials Science and Engineering, Hainan University, Haikou, China, [2] Suzhou Institute of Nano-Tech and Nano-Bionics, Chinese Academy of Sciences, Suzhou, China, [3] Division of Surgery and Interventional Science, University College London, London, United Kingdom

OPEN ACCESS

Edited by:
Pingan Song,
University of Southern Queensland, Australia

Reviewed by:
Song He,
Wuhan University of Technology, China
Wei Wei,
Jiangsu University, China
Hyung-Ho Park,
Yonsei University, South Korea

***Correspondence:**
Jin Wang
jwang2014@sinano.ac.cn
Jianhe Liao
990359@hainanu.edu.cn
Xuetong Zhang
xtzhang2013@sinano.ac.cn

Specialty section:
This article was submitted to Polymeric and Composite Materials, a section of the journal Frontiers in Materials

Received: *28 January 2021*
Accepted: *24 March 2021*
Published: *27 April 2021*

Citation:
Liu R, Wang J, Liao J and Zhang X (2021) Robust Silica–Polyimide Aerogel Blanket for Water-Proof and Flame-Retardant Self-Floating Artificial Island. Front. Mater. 8:659655. doi: 10.3389/fmats.2021.659655

A robust silica–polyimide (PI) aerogel blanket is designed and synthesized using the PI foam as the matrix and silica aerogel as the filler through an *in situ* method, where sol–gel transition of silica precursor occurs in pores of the PI foam, followed by the hydrophobization and ambient pressure drying. The density of the aerogel blanket ranges from 0.036 to 0.196 g/cm^3, and the low density is directly controlled by tailoring the silica concentration. The specific surface area of the aerogel blanket reaches 728 m^2/g. These features of the blanket result in a low thermal conductivity of 0.018 W/mK, which shows a remarkable reduction of 59% compared to that of the PI foam (0.044 W/mK). As a result, a remarkable decrease of 138°C is achieved using the silica blanket as the thermal insulator on a hot plate of approximately 250°C. In addition, the temperature degradation of the blanket is around 500°C, and up to 86% of mass remaining at 900°C is obtained. The blanket is resistant at extremely harsh conditions, e.g., 600°C for 30 min and 1,300°C for 1 min, and no open flame is observed, suggesting a significant flame-retardant of the blanket. Owing to the three-dimensional (3D) porous framework of the PI foam, the silica aerogel is encapsulated in the PI foam and the blanket exhibits strong mechanical property. The silica–PI aerogel can be reversibly compressed for 50 cycles without reduction of strain. The contact angle of the blanket is 153°, which shows a superior waterproof property. Combining with the low density, low thermal conductivity, flame-retardant, and strong mechanical strength, the aerogel blanket has the potential as an artificial island, which is safe (waterproof and flame-retardant), lightweight, comfortable, and easy to be moved.

Keywords: silica, polyimide, self-floating, aerogel blanket, artificial island

INTRODUCTION

Aerogels are the type of nanoporous materials possessing extremely low density, low thermal conductivity, high porosity, and high pore volume, and are potentially used in various fields such as environment, energy, cosmetic, transportation, building, catalyst, and biomedicine (Koebel et al., 2012; Ziegler et al., 2017; Vareda et al., 2018; Qie et al., 2020; Wei et al., 2020;

Wang and Wang, 2021). Among a variety of aerogels, silica aerogels are the most frequently used aerogels owing to their relatively low price, ease of scale-up, and excellent overall properties (Du et al., 2013; Wang and Zhang, 2015; Chen et al., 2017; Wang et al., 2017, 2018; Li T. et al., 2018; Li X. et al., 2018). However, silica aerogels are very brittle, which inhibits their wide applications (Wong et al., 2014; Liu et al., 2019). Strategies to improve the mechanical property of silica aerogels have been proposed by several research groups. As illustrated in **Figure 1A**, one of the most effective methods is the modification of silica networks with different organic groups or polymers (Liu Z. et al., 2020). For example, hybrid silica aerogels prepared from organic group-bridged silica precursors (Boday et al., 2011; Wang et al., 2013; Wang Z. et al., 2015; Wei et al., 2015; Yun et al., 2015; Zhang et al., 2017) were robust and could be compressed up to 80% without any damage. Silica aerogels synthesized from vinyl-functionalized siloxanes were build up with organic–inorganic double cross-linking networks, and they exhibited remarkable mechanical strength, flexibility, and is capable of ambient pressure drying (APD; Shimizu et al., 2016, 2017; Zu et al., 2018a,b,c). However, these approaches involve expensive monomers, complicated synthetic processes, and their scale-up productions are yet to be reported. Another strategy is introducing fibers to synthesize silica aerogel blankets (**Figure 1A-2**), which results in the flexible aerogel blanket that could be bent using polyester and glass fibers as a matrix (Berardi and Zaidi, 2019; Berthon-Fabry et al., 2017; Huang et al., 2019; Talebi et al., 2019; Lakatos, 2019). Though this approach is able to scale-up and commercially available, the interaction between silica aerogel and the fibrous matrix is weak, and the silica aerogel in the blanket can still be cracked and becomes ineffective.

To solve the problems, a silica–polyimide (PI) foam aerogel blanket is proposed as shown in **Figure 1A-3**, where the brittle silica aerogel is encapsulated in the three-dimensional (3D) framework of PI foam. Even though the interaction between the silica aerogel and the PI network is weak, the silica aerogel is less possible to drop out from the blanket owing to the encapsulation effect. Indeed, various silica–PI composite aerogels have been synthesized *via* different approaches, and all of them show excellent flame-retardant performances (Fan et al., 2019; Sun et al., 2020; Zhang et al., 2020; Wu et al., 2021), which indicated that the combination of PI and silica would be an effective way to improve the performance of native silica aerogels. Thus, the proposed method to synthesize the silica–PI aerogel foam blankets cannot only significantly improve its properties, but it is also possible to synthesize the aerogel blanket *via* a one-pot process (**Figure 1B**). In this work, the synthetic parameters, physical properties including mechanical strength, thermal stability, hydrophobicity, etc., will be investigated. The relationship between structure and property will also be highlighted. Considering the scale production and excellent overall properties, the silica–PI aerogel blanket will be an ideal candidate for the construction of artificial islands (**Figure 1C**), which is self-floating, waterproof, flame-retardant, lightweight, and thermal insulation, leading to a safe and comfortable floating platform for emergency event application.

MATERIALS AND METHODS

Materials

Tetraethoxysilane (TEOS, AR), hexane (AR), hydrochloric acid (36–38 wt.%), ammonia aqueous solution (25–28 wt.%), and ethanol (≥99.7%, AR) were purchased from the Sinopharm Chemical Reagent Co., Ltd. (Shanghai, China). Trimethylchlorosilane (TMCS, 98%) was purchased from Nanjing HaBo Medical Technology Co., Ltd. (Nanjing, China). Condensed silica solutions (CS) were synthesized in advance as the silica precursors in accordance with our previous work (Wang et al., 2014; Wang J. et al., 2015, 2016), the molar ratio of TEOS:ethanol:HCl (10^{-2} mol/L) is 1:4:1.2. All other reagents and PI foam were used without further purification.

Synthesis of Silica–PI Aerogel Blankets

The synthetic process of silica–PI aerogel blankets was shown in **Figure 1B**. The specific steps are as follows: take the sample SAF-1 as an example, the volume of PI foam was 800 cm^3 (20 cm × 20 cm × 2 cm), 1 L of silica precursors solution was prepared by adding 160 mL of CS to 840 mL ethanol, and the content of SiO_2 was diluted to 20 mg/mL (the content of SiO_2 in CS solution was 125 mg/mL). The mixture was stirred for 5 min, and 10 mL of ammonia aqueous solution was added under stirring. Then, the PI foam was immersed in the mixture and stood still until the CS solution in the PI foam was gelled. The composite gel was aged at room temperature for 8 h and went through solvent exchange with hexane for a week. Then, 50 mL of TMCS were added to a hydrophobically modified silica gel for 1 day. Finally, the modified blanket was dried at 150°C for 3 h under ambient pressure. The silica–PI aerogel blanket was called as SAF-n, where n is 1, 2, 3, 4, 5, and 6, corresponding to the silica content in the diluted CS solution of 20, 40, 60, 80, 100, and 0 mg/mL.

Characterizations

The average pore size and distribution of the silica–PI aerogel blanket were evaluated by the BJH method (ASAP 2020, Micromeritics, United States). Cumulative pore volume was measured at the point $P/P_0 = 0.99$. The SA of the SiO_2 aerogel was figured out by the Brunauer–Emmett–Teller (BET) method, and the data were collected at pressures (P/P_0) from 0.05 to 0.3.

The thermal conductivity was determined with an HFM 436/3/1E Thermal Conductivity Tester (Netzsch, Germany) and the temperature was set to 25°C.

Thermogravimetric analysis (TGA) was measured on TG 209F1 Libra (NETZSCH) analyzer with a ramp rate of 10°C/min under nitrogen.

The water contact angle was characterized using OCA 15EC, Data Physics Instruments GmbH.

The FTIR spectrum was measured by Fourier infrared spectrometer (Nicolet 6700, Thermo Fisher Scientific, United States), and the samples were ground together with KBr and then pressed into a thin sheet for testing.

For the thermal insulation test, a ceramic hot plate was used as the heat source, and the silica–PI aerogel

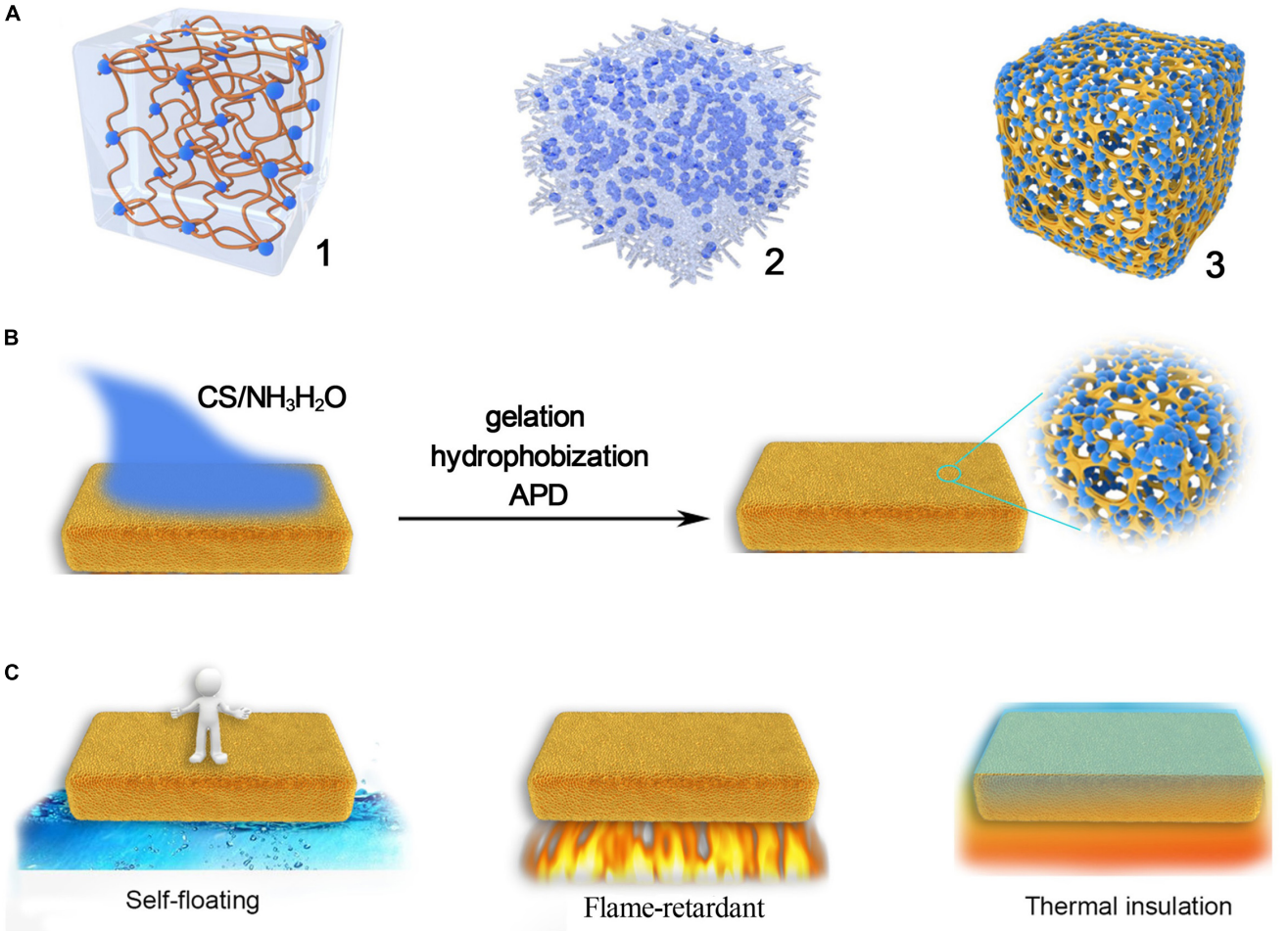

FIGURE 1 | (A) Mechanical enhancement of the silica aerogel by organic groups or polymers (1), silica aerogel blanket (2), and proposed structure of silica foam blanket (3), **(B)** schematic description of the *in situ* synthesis of silica–PI aerogel blanket, and **(C)** properties of the aerogel blanket and potential applications.

was heated by a DC stabilized power supply (2280S-60-3, Keithley, United States). The current was set to 3 A, and the voltage was set to 15 V. Samples with 5 mm thickness was placed on the hot plate, a multichannel data recorder (TP9000, Toprie, China) connected to a K-type thermocouple was used to test the real-time temperature of the top layer of the sample with a measurement interval of 1 s. The infrared thermal images were taken using an infrared camera (TiX580, Fluke). Infrared thermal images and temperature–time curves were collected in an open environment with thermal convection and thermal radiation, which dissipated the heat naturally.

The compressive stress–strain measurement was performed on an Instron 3365 tensile testing machine, and the compression speed was 5 mm/min. The strain increased from 20 to 50% in the loading–unloading cycles.

The limiting oxygen index (LOI) of the silica–PI aerogel blanket was analyzed by the Limiting Oxygen Index Instrument (FTT0077 Co., Ltd., United Kingdom), and the size of the sample was 80 mm × (10 ± 0.5 mm) with the thickness of 8 mm.

RESULTS AND DISCUSSION

Silica–PI aerogel blankets were synthesized through a one-step process as shown in **Figure 1B**. Ammonia aqueous solution was mixed in the CS solution with a predetermined concentration. PI foam was then immersed in the CS solution. Aerogel blankets were obtained after gelation, hydrophobization, and APD. As presented in **Figure 2A**, a large PI foam with a size of 30 cm × 30 cm × 4 cm can be successfully converted into the silica–PI aerogel blanket (**Figure 2B**) with no visible volume shrinkage. The density of the PI foam was 9 mg/cm^3, while that of aerogel blankets were 36, 69, 81, 118, and 196 mg/cm^3, respectively. The densities of the blankets showed a direct correlation with CS concentration. The thermal conductivity of the aerogel blankets ranged from 0.018 to 0.033 W/mK, which was dependent on density, in which SAF-3 with a density of 81 mg/cm^3 exhibited the lowest thermal conductivity of 0.018 W/mK and SAF-5 with a density of 196 mg/cm^3 had the highest thermal conductivity of 0.033 W/mK. The SEM image of the PI foam (**Figure 2C**) revealed an interconnected porous

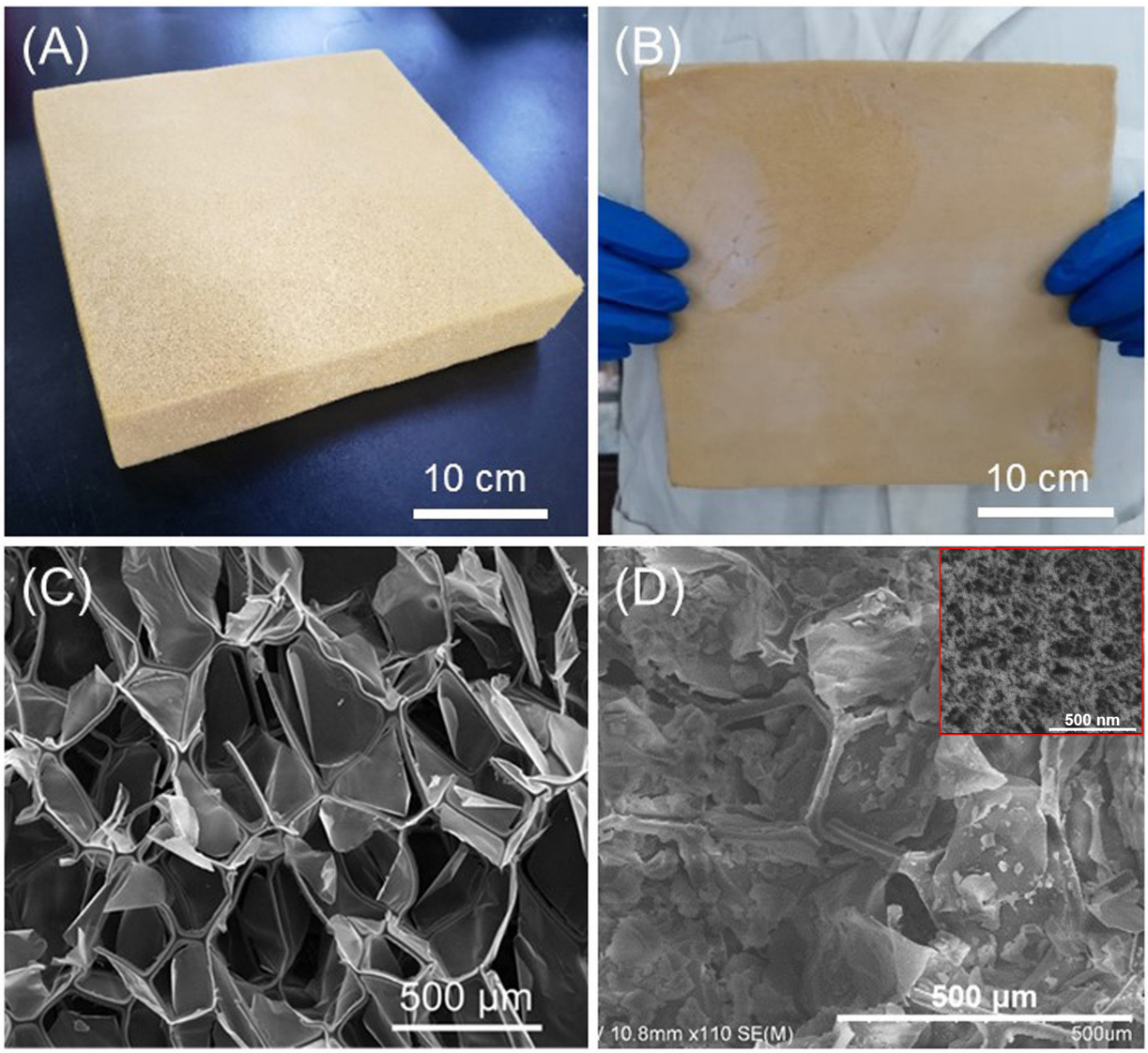

FIGURE 2 | Optical images of PI foam **(A)** and silica–PI aerogel blanket, SAF-3 **(B)**, SEM images of PI foam **(C)**, and silica–PI aerogel blanket (inset is the nanoscale image of silica aerogel), SAF-3 **(D)**.

structure with a 3D framework. The diameter of the pores ranged from 400 to 500 μm. Both the silica aerogel and PI framework in the blanket could be observed (**Figure 2D**), and they were closely contacted without a large crack (**Supplementary Figure 1**), indicating that the silica aerogel had been completely filled in by the pores. Thus, the remarkable reduction of the thermal conductivity of PI foam (0.044 W/mK) may be due to the silica aerogels, in which the air in the macropores of the foams was replaced by silica aerogels. Consequently, the thermal conductivity attributed by air convection was suppressed.

Figure 3A shows the FTIR spectra of the aerogel blankets. The vibration peaks of Si–O–Si and Si–C can be observed at 1100 and 840 cm^{-1}, respectively, which indicated the presence of silica aerogels. Besides, vibration peaks located at ca. 2,980 and 2,982 cm^{-1} can be clearly observed, which could be ascribed to the vibration of C–H bonds from the $–CH_3$ and $–CH_2CH_3$ groups. The results confirmed the successful hydrophobization of the silica gel, which was a critical point toward APD (Prakashi et al., 1995; Yun et al., 2014; Li Y. et al., 2018). In addition, the characteristic peaks of PI located at 1,714 and 1,771 cm^{-1} (C=O), 1,370 cm^{-1} (C–N), and 1,496 cm^{-1} (C=C) could be observed in all the blankets, with no change compared with PI foam, suggesting that the *in situ* synthetic process (including the hydrophobization) did not influence the chemical structure of the PI matrix. **Figures 3B,C** show the N_2 adsorption–desorption isotherms and the pore size distribution curves of the aerogel blankets. All the blankets exhibited hysteresis loops, which were due to the characteristic features of mesoporous materials (type IV isotherms). The BET surface areas of the samples ranged from 573 to 728 m^2/g depending on density. The average pore size of

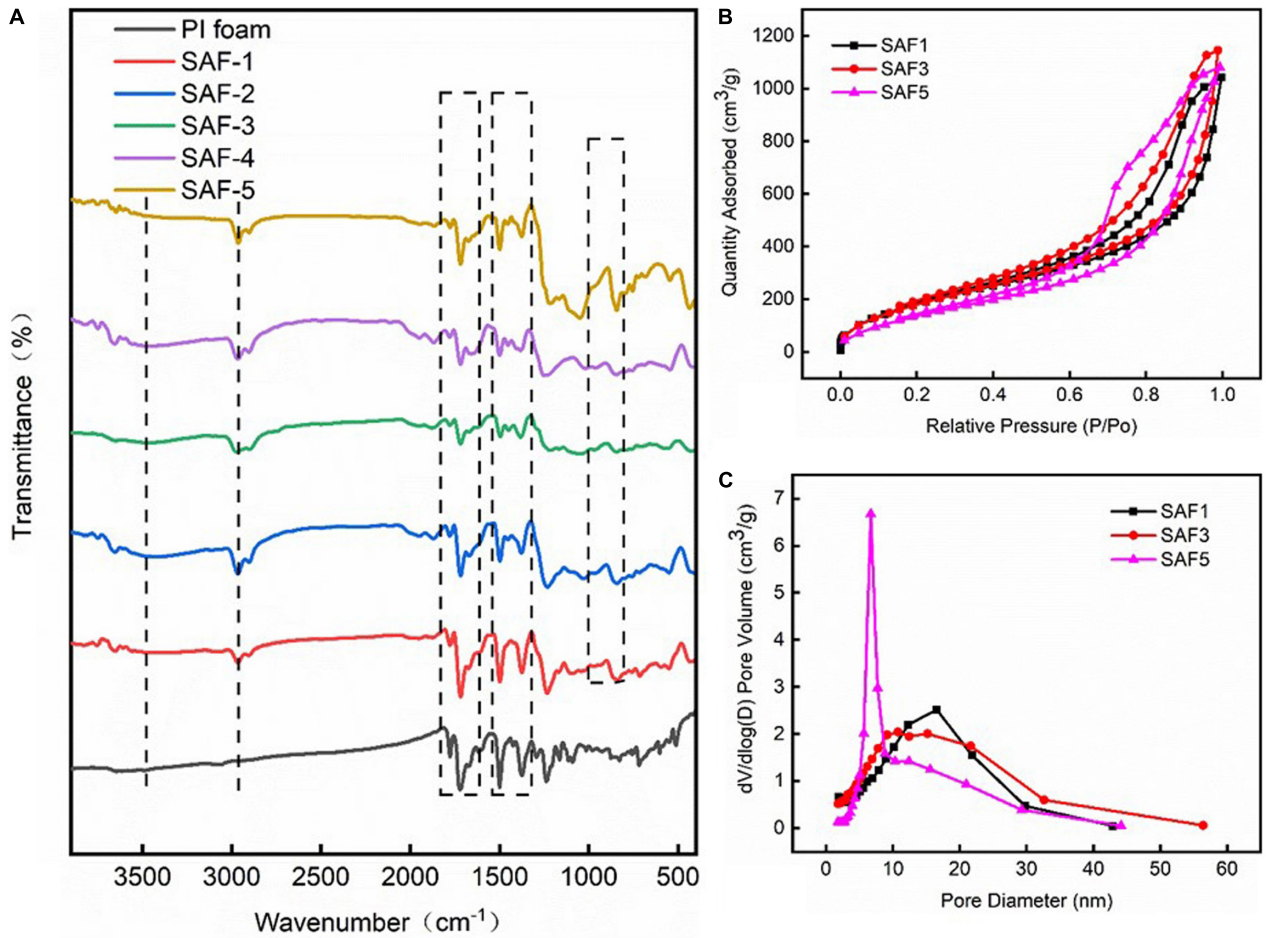

FIGURE 3 | (A) FTIR spectra of the PI foam and silica–PI aerogel blankets, **(B)** nitrogen adsorption–desorption isotherms of the silica–PI aerogel blanket as indicated, and **(C)** pore size distribution of the silica–PI aerogel blankets.

the aerogel blankets (7–20 nm) also showed a reliance on density, which decreased with the increase in density.

Figure 4A and **Supplementary Figure 2A** show the compressive–stress curves of PI foam and the silica–PI aerogel blankets. The PI foam could be compressed up to 85% and the recovery from the deformation, modulus of PI foam was 0.36 KPa. The blankets with lower densities, e.g., SAF-1, SAF-2, and SAF-3 could be compressed up to 80%, while those with higher densities were broken with a small strain of less than 40%. The modulus of the blankets ranged from 0.4 to1.8 KPa, which was remarkably increased when compared to the pure PI foam (0.36 KPa). Pure silica aerogel monoliths have been reported to be broken at a strain of 10% (Jiang et al., 2017). Thus, the encapsulation of silica aerogels with a 3D foam was an effective method to improve their mechanical properties. In addition, the robustness of the blankets can be reflected from the loading–unloading compression study. As shown in **Figure 4B**, SAF-3 could be reversibly compressed up to 40% strain, and the curves during loading were overlapped when the strain was lower than 40%. When the blanket was compressed to 50%, the blanket can also be completely recovered by suggesting that the silica aerogels were stable in the blankets, though the modulus decreased. The time–strain and time–stress curves (**Figure 4C**) of the compression test during 50 loading–unloading cycles at 30% strain for SAF-3 further indicated that the silica aerogel blankets using a PI foam matrix showed a significant improvement in the mechanical properties. The stress of the blankets did not decrease even after 50 cycles of compression. The results confirmed that using a 3D porous structure as the matrix was a robust strategy to synthesize mechanically stable silica-based aerogel blankets. Interestingly, as shown in **Supplementary Figure 2B**, SAF-3 after burning at 600°C for 30 min could be reversibly compressed up to 20% strain, and the curves during loading were overlapped when the strain was lower than 30%, which indicated that the mechanical property of the blanket could be preserved to a certain extent. Nevertheless, they could not be reversibly compressed higher than 30% strain, which indicated that the PI matrix would be destroyed, as will be discussed in the following section.

Silica aerogels cannot be burned, but silica aerogel blanket using polymer-based fibers as the matrix showed a poor fireproofing grade, which severely restricts their applications (Berardi and Zaidi, 2019). On the other hand, PI is a kind of

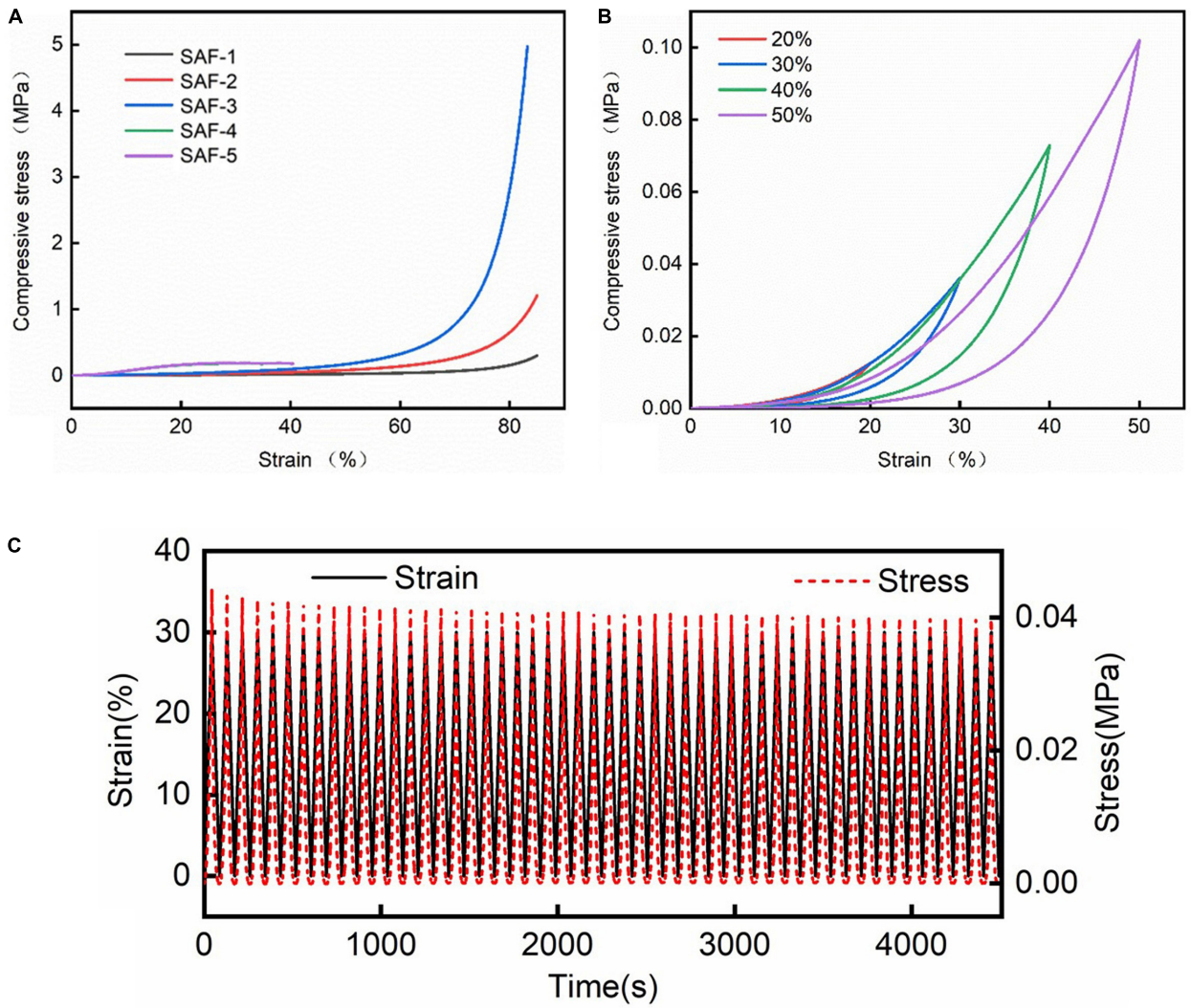

FIGURE 4 | (A) Compressive strain–stress curves of the silica–PI aerogel blankets, **(B)** compressive strain–stress curves of SAF-3 during loading–unloading cycles at ε = 20, 30, 40, and 50%. **(C)** The time–strain and time–stress curves of the compression test during 50 loading–unloading cycles at 30% strain for SAF-3.

polymer with high thermal stability and most of them are non-flammable (Liu H. et al., 2020). Therefore, the silica–PI aerogel blankets designed in this work show excellent flame-retardant properties. As presented in **Figures 5A,B**, the IP foam could not get burned, but it was damaged and completely distorted under a flame of 1,300°C for 1 min. On the contrary, the silica–PI aerogel blankets showed much more stability at the same condition (a flame of 1,300°C for 1 min) (**Figures 5C,D**), and all the silica aerogels were kept intact though the PI foam matrix had been thermally degraded (**Supplementary Figure 3**). When the silica–PI aerogel blanket was presented on an alcohol burner at 600°C, only the surface of the aerogel blanket was burned (**Figures 5E,F**). The LOI of the aerogel blanket (SAF-3) was 34%. The results indicated that the silica–PI aerogels possessed remarkable flame-retardant properties. The IR image of the blanket and PI foam was shown in **Figures 5G,H**. Clearly, with the same thickness, the temperature of the upper surface of the blanket was lower than that of the PI foam. Moreover, when the aerogel blanket was presented on a hot plate at 250°C, the temperature of the upper surface of the blanket was ca. 138°C, which is lower than that of the hot plate. However, when the bare PI foam was placed on the hot plate, the temperature of the foam surface was 94°C, which is lower than that of the temperature of the hot plate. It can be seen that aerogel blankets exhibited better thermal insulation capacity than PI foam when compared to pure silica aerogels (Du et al., 2020; **Figure 5I**). The thermal stability of the silica–PI aerogel blankets was also similar to that of the PI foam, where the decomposition temperature of the blanket and foam at 5% was ca. 500°C (**Figure 5J**). The mass decline of the silica blankets below 600°C would mainly contribute to the degradation of side groups of PI, while the sharp decline over 600°C must be due to the decomposition of the backbone of PI. Besides, the degradation of Si–CH_3 and Si–OH groups in the silica aerogels also occurred when the temperature was

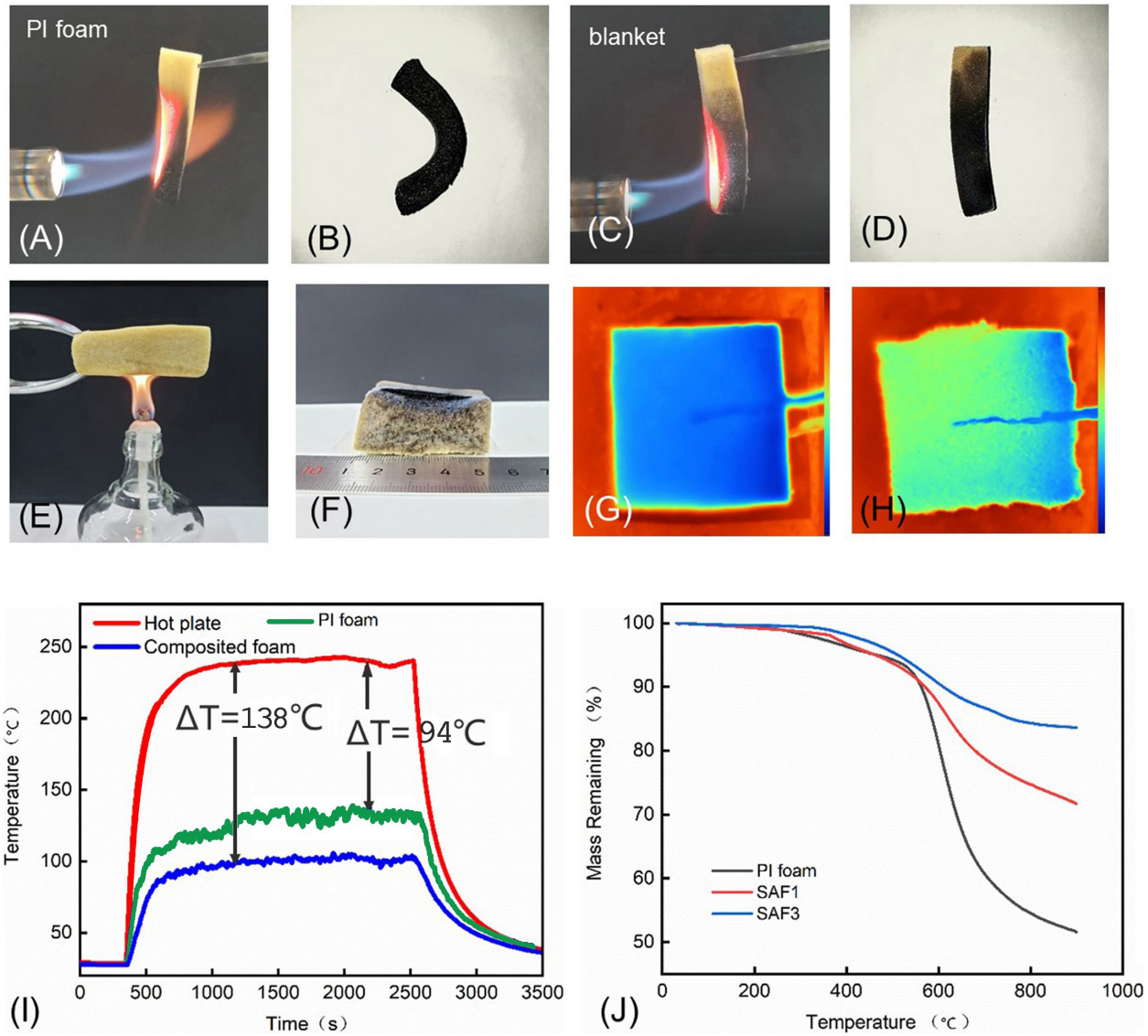

FIGURE 5 | Optical images of PI foam before **(A)** and after **(B)** combustion under fire of 1,300°C for 1 min. Photo images of silica–PI aerogels blanket (SAF-3) before **(C)** and after **(D)** combustion under fire of 1,300°C for 1 min. Optical images of silica–PI aerogels blanket (SAF-3) before **(E)** and after **(F)** combustion under fire of 600°C for 30 min. **(G)** The IR image of SAF3 on a hot plate at 250°C. **(H)** The IR image of PI foam on a hot plate at 250°C. **(I)** Time–temperature curves of the hot plate and the upper surface of the PI foam and aerogel blanket (SAF-3) on the hot plate. **(J)** TGA traces of PI foam, SAF-1, and SAF-3.

higher than 350°C (He et al., 2019). However, due to the small fraction of the $-CH_3$ and –OH groups when compared to PI, the mass decline of the two groups was not obvious in the TGA curves. The residue mass of the blanket at 900°C was much higher than that of PI foam. For example, the mass remaining value of SAF-1 and SAF-3 was 74 and 86%, respectively (which suggested that the mass residue increased with the increase in silica aerogels). While that of PI foam was only 50%. The results discussed above indicated that silica aerogels encapsulated in the PI foam can significantly increase both the flame-retardant and thermal stability of the aerogel blanket.

The densities of the silica–PI aerogel blankets are shown in **Figure 6A**. The direct relationship between density and the CS concentration indicated that the density could be varied by CS concentration. The highest density was 196 mg/cm^3 for SAF-5 with a CS concentration of 0.1 g/cm^3. Interestingly, the blankets were superhydrophobic with the contact angle higher than 150°, which was a significant increase when compared to the hydrophobic property of PI foam (**Figures 6B,C**). Owing to the superhydrophobic property and low density, the aerogel blankets could be used as an ideal self-floating platform on the water. In general, an artificial floating island is a eutrophic water purification technology used for decontamination and ecological remediation due to the landscape effects. It works as a natural evolution of artificial wetlands or green filters, which has a history of nearly 40 years (Kong et al., 2019; Largo et al., 2020;

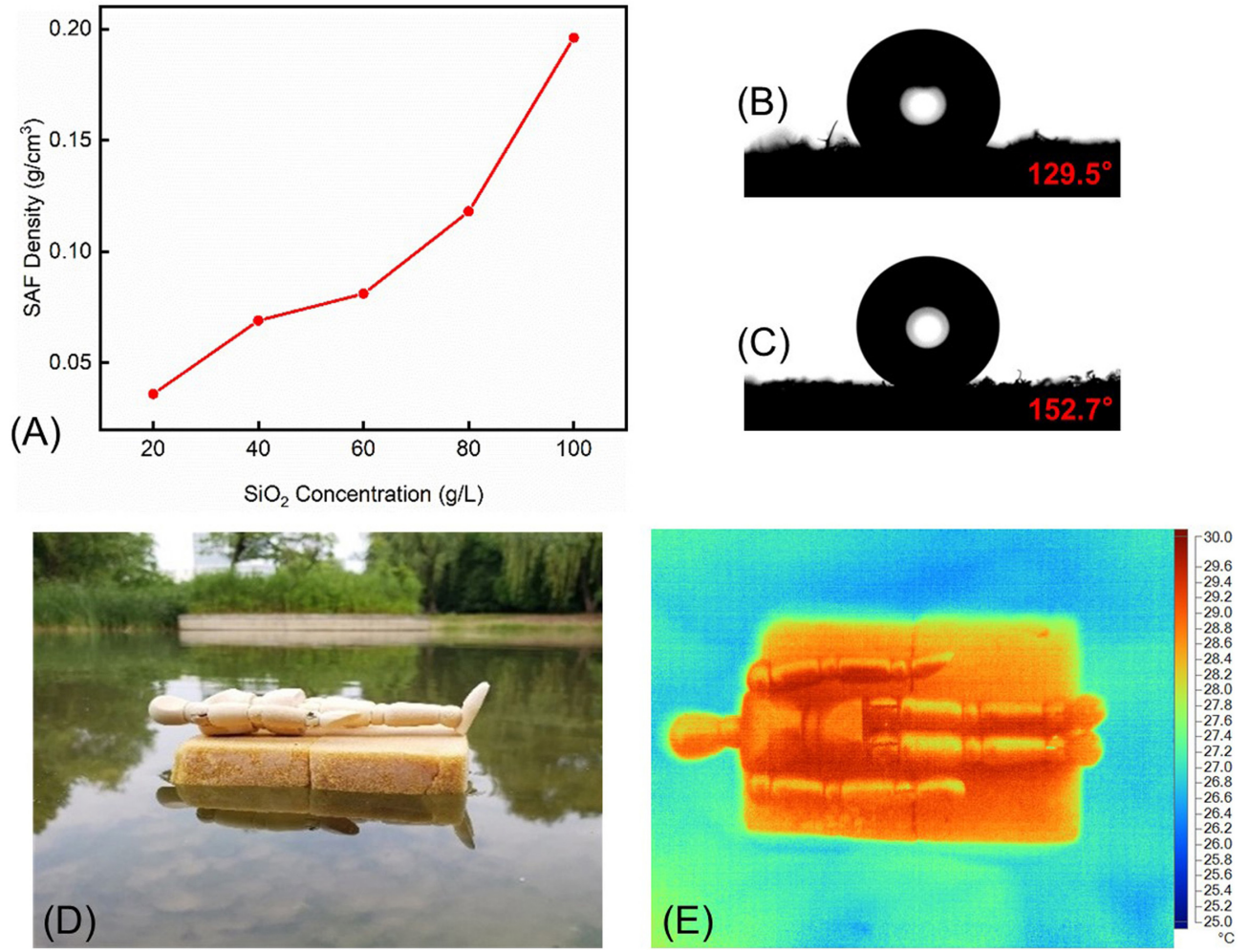

FIGURE 6 | (A) CS concentration and density cure of the aerogel blanket, **(B)** contact angle image of the PI foam, **(C)** contact angle image of silica–PI aerogel blanket, SAF-3, **(D)** photo image, and **(E)** IR image of the aerogel blanket as self-floating island carrying a dummy.

Prashant and Billore, 2020; Ren et al., 2021). In this work, the aerogel blankets could be used as self-floating islands and as movable platforms for supporting or transporting goods and materials, rather than constructions for water purification. Considering the complicated condition on water, such as cold lake and sea, burning crude oil that was leaked, the requirement of working platforms on the water for a long-term period makes the silica–PI aerogel blankets as potential artificial islands. It should also be flame-retardant that meets the requirements of excellent thermal insulation properties and long-term stability, which is not only safe and comfortable but also easily movable on water due to their low density and superhydrophobicity (that may reduce the force of friction). As a primary study, an aerogel blanket was presented on a lake, and it can self-float on water (**Figure 6D**). An IR image was taken after putting a dummy on the blanket (**Figure 6E**). It could be seen clearly that both the aerogel blanket and the dummy possessed a temperature of ca. 4°C higher than that of the water surface, which indicated that the artificial island not only acts as a floating platform on the water but also shows excellent thermal insulation property due to their extremely low thermal conductivity (<0.03 W/mK).

CONCLUSION

In sum, a robust silica–PI aerogel blanket is designed and synthesized using an *in situ* method based on PI foam. The density of the aerogel blanket can be directly controlled using different CS concentrations, and the extremely low thermal conductivity of 0.018 W/mK is achieved and a remarkable temperature difference of 138°C is achieved using the blanket as a thermal insulator on a hot plate of approximately 250°C. Owing to the 3D porous framework of PI foam, the silica aerogel is encapsulated and the blankets exhibit strong mechanical properties, and they can be reversibly compressed for 50 cycles without reduction of strain. Moreover, the silica aerogel possesses a high degradation temperature of 500°C, and is resistant to extremely harsh conditions, e.g., 600°C for 30 min

and 1300°C for 1 min. In addition, the contact angle of the blanket is 152°. Combining with the low density, low thermal conductivity, flame-retardant, and strong mechanical strength of the aerogel blanket, the silica–PI aerogel blanket has significant and commercial potential as the artificial islands that are safe, lightweight, comfortable, and easy to move.

DATA AVAILABILITY STATEMENT

The original contributions presented in the study are included in the article/**Supplementary Material**, further inquiries can be directed to the corresponding authors.

AUTHOR CONTRIBUTIONS

RL performed the experiments and summarized the data. JW designed the experiment, supervised, and wrote the manuscript. JL and XZ supervised the projects and comments on the manuscript. All authors contributed to the article and approved the submitted version.

FUNDING

This work was financially supported by the National Natural Science Foundation of China (91963124 and 51773225) and the Royal Society Newton Advanced Fellowship (NA170184).

SUPPLEMENTARY MATERIAL

The Supplementary Material for this article can be found online at: https://www.frontiersin.org/articles/10.3389/fmats.2021.659655/full#supplementary-material

REFERENCES

Berardi, U., and Zaidi, S. M., (2019). Characterization of commercial aerogelenhanced blankets obtained with supercritical drying and of a new ambient pressure drying blanket. *Energy Build.* 198, 542–552. doi: 10.1016/j.enbuild.2019.06.027

Berthon-Fabry, S., Hildenbrand, C., Ilbizian, P., Jones, E., and Tavera, S. (2017). Evaluation of lightweight and flexible insulating aerogel blankets based on resorcinol-formaldehyde-silica for space applications. *Eur. Polym. J.* 93, 403–416. doi: 10.1016/j.eurpolymj.2017.06.009

Boday, D. J., Stover, R. J., Muriithi, B., and Loy, D. A. (2011). Strong, low density, hexylene- and phenylene-bridged polysilsesquioxane aerogel-polycyanoacrylate composites. *J. Mater. Sci.* 46, 6371–6377. doi: 10.1007/s10853-011-5584-7

Chen, Y., Shao, G., Hong, Y., Shen, X., and Cui, S. (2017). Facile preparation of cross-linked polyimide aerogels with carboxylic functionalization for CO2 capture. *Chem. Eng. J.* 322, 1–9. doi: 10.1016/j.cej.2017.04.003

Du, A., Zhou, B., Zhang, Z., and Shen, J. (2013). A special material or a new state of matter: a review and reconsideration of the aerogel. *Materials* 6, 941–968. doi: 10.3390/ma6030941

Du, Y., Zhang, X., Wang, J., Liu, Z., Zhang, K., Ji, X., et al. (2020). Reaction-spun transparent silica aerogel fibers. *ACS Nano* 14, 11919–11928. doi: 10.1021/acsnano.0c05016

Fan, W., Zhang, X., Zhang, Y., Zhang, Y., and Liu, T. (2019). Lightweight, strong, and super-thermal insulating polyimide composite aerogels under high temperature. *Comp. Sci. Tech.* 173, 47–52. doi: 10.1016/j.compscitech.2019.01.025

He, S., Huang, Y., Chen, G., Feng, M., Dai, H., Yuan, B., et al. (2019). Effect of heat treatment on hydrophobic silica aerogel. *J. Hazard. Mater.* 362, 294–302. doi: 10.1016/j.jhazmat.2018.08.087

Huang, Y., He, S., Chen, G., Dai, H., Yuan, B., Chen, X., et al. (2019). Fast preparation of glass fiber/silica aerogel blanket in ethanol and water solvent system. *J. Non Crystal. Solids* 505, 286–291. doi: 10.1016/j.jnoncrysol.2018.11.003

Jiang, L., Kato, K., Mayumi, K., Yokayama, H., and Ito, K. (2017). One-pot synthesis and characterization of polyrotaxane-silica hybrid aerogel. *ACS Macro Lett.* 6, 281–286. doi: 10.1021/acsmacrolett.7b00014

Koebel, M., Rigacci, A., and Achard, P. (2012). Aerogel-based thermal superinsulation: an overview. *J. Sol Gel Sci. Technol.* 63, 215–339.

Kong, L., Wang, L., Wang, Q., Mei, R., and Yang, Y. (2019). Study on new artificial floating island removing pollutants. *Environ. Sic. Pollut. Res.* 26, 17751–17761. doi: 10.1007/s11356-019-05164-4

Lakatos, Á (2019). Stability investigations of the thermal insulating performance of aerogel blanket. *Energy Build.* 185, 103–111. doi: 10.1016/j.enbuild.2018.12.029

Largo, K. M. F., Depablos, J. L. R., Espitia-Sarmiento, E. F., and Moreta, N. M. L. (2020). Artificial floating island with Vetiver for treatment of arsenic-contaminated water: a real scale study in high-andean reservoir. *Water* 12:3086. doi: 10.3390/w12113086

Li, T., Du, A., Zhang, T., Ding, W., Liu, M., Shen, J., et al. (2018). Efficient preparation of crack-free, low-density and transparent polymethylsilsesquioxane aerogels via ambient pressure drying and surface modification. *RSC Adv.* 8, 17967–17975. doi: 10.1039/c8ra03061h

Li, X., Wang, J., Zhao, Y., and Zhang, X. (2018). Template-free self-assembly of fluorine-free hydrophobic polyimide aerogels with lotus or petal effect. *ACS Appl. Mater. Interfaces* 10, 16901–16910. doi: 10.1021/acsami.8b04081

Li, Y., Du, A., Shen, J., Zhang, Z., Wu, G., and Zhou, B. (2018). Temperature dependence of dynamic mechanical behaviors in low density MTMS-derived silica aerogel. *J. Porous Mater.* 25, 1229–1235. doi: 10.1007/s10934-017-0533-8

Liu, H., Tian, H., Yao, Y., Xiang, A., Qi, H., Wu, Q., et al. (2020). Polyimide foams with outstanding flame resistance and mechanical properties by the incorporation of noncovalent bond modified graphene oxide. *New J. Chem.* 44, 12068–12078. doi: 10.1039/d0nj01983f

Liu, R., Wang, J., Du, Y., Liao, J., and Zhang, X. (2019). Phase-separation induced synthesis of superhydrophobic silica aerogel powders and granules. *J. Solid State Chem.* 279:120971. doi: 10.1016/j.jssc.2019.120971

Liu, Z., Ran, Y., Xi, J., and Wang, J. (2020). Polymeric hybrid aerogels and their biomedical applications. *Soft. Matter.* 16, 9160–9175. doi: 10.1039/d0sm01261k

Prakashi, S. S., Brinker, C. J., and Hurd, A. J. (1995). Silica aerogel films at ambient pressure. *J. Non Crystal. Solids* 190, 264–275. doi: 10.1016/0022-3093(95)00024-0

Prashant, and Billore, S. K. (2020). Macroinvertebrates associated with artificial floating islands installed in River Kshipra for water quality improvement. *Water Sci. Tech.* 81, 1242–1249. doi: 10.2166/wst.2020.219

Qie, S., Hao, Y., Liu, Z., Wang, J., and Xi, J. (2020). Advances in cyclodextrin polymers and their applications in biomedicine. *Acta Chim. Sin.* 78, 232–244. doi: 10.6023/a20010006

Ren, P., Zhu, H., Sun, Z., and Wang, C. (2021). Effects of artificial islands construction on the spatial distribution and risk assessment of heavy metals in the surface sediments from a semi-closed bay (Longkou Bay), China. *Bull. Environ. Contamin. Toxic.* 105, 44–50. doi: 10.1007/s00128-020-03032-3

Shimizu, T., Kanamori, K., Maeno, A., Kaji, H., Doherty, C. M., Falcaro, P., et al. (2016). Transparent, highly insulating polyethyl- and polyvinylsilsesquioxane aerogels: mechanical improvements by vulcanization for ambient pressure drying. *Chem. Mater.* 28, 6860–6868. doi: 10.1021/acs.chemmater.6b01936

Shimizu, T., Kanamori, K., Maeno, A., Kaji, H., Doherty, C. M., and Nakanishi, K. (2017). Transparent ethenylene-bridged polymethylsiloxane aerogels: mechanical flexibility and strength and availability for addition reaction. *Langmuir* 33, 4543–4550. doi: 10.1021/acs.langmuir.7b00434

Sun, G., Duan, T., Liu, C., Zhang, L., Chen, R., Wang, J., et al. (2020). Fabrication of flame-retardant and smoke-suppressant isocyanate-based polyimide foam modified by silica aerogel thermal insulation and flame protection layers. *Polym. Testing* 91:106738. doi: 10.1016/j.polymertesting.2020.106738

Talebi, Z., Soltani, P., Habibi, N., and Latifi, F. (2019). Silica aerogel/polyester blankets for efficient sound absorption in buildings. *Constr. Build. Mater.* 220, 76–89. doi: 10.1016/j.conbuildmat.2019.06.031

Vareda, J. P., Lamy-Mendes, A., and Durães, L. (2018). A reconsideration on the definition of the term aerogel based on current drying trends. *Micropor. Mesopor. Mater.* 258, 211–216. doi: 10.1016/j.micromeso.2017.09.016

Wang, J., Du, R., and Zhang, X. (2018). Thermoresponsive polyrotaxane aerogels: converting molecular necklaces into tough porous monoliths. *ACS Appl. Mater. Interfaces* 10, 1468–1473. doi: 10.1021/acsami.7b18741

Wang, J., and Wang, J. (2021). Advances on dimensional structure design and functional applications of aerogels. *Acta Chim. Sin.* [Epub ahead of print]. doi: 10.6023/A20110531

Wang, J., Wang, X., and Zhang, X. (2017). Cyclic molecule aerogels: a robust cyclodextrin monolith with hierarchically porous structures for removal of micropollutants from water. *J. Mater. Chem. A* 5, 4308–4313. doi: 10.1039/c6ta09677h

Wang, J., Wei, Y., He, W., and Zhang, X. (2014). A versatile ambient pressure drying approach to synthesize silica-based composite aerogels. *RSC Adv.* 4, 51146–51155. doi: 10.1039/c4ra10607e

Wang, J., and Zhang, X. (2015). Binary crystallized supramolecular aerogels derived from host-guest inclusion complexes. *ACS Nano* 9, 11389–11397. doi: 10.1021/acsnano.5b05281

Wang, J., Zhang, Y., Wei, Y., and Zhang, X. (2015). Fast and one-pot synthesis of silica aerogels via a quasi-solventexchange-free ambient pressure drying process. *Micropor. Mesopor. Mater.* 218, 192–198. doi: 10.1016/j.micromeso.2015.07.019

Wang, J., Zhang, Y., and Zhang, X. (2016). Reversible superhydrophobic coatings on lifeless and biotic surfaces via dry-painting of aerogel microparticles. *J. Mater. Chem. A* 4, 11408–11415. doi: 10.1039/c6ta04306b

Wang, Z., Dai, Z., Wu, J., Zhao, N., and Xu, J. (2013). Vacuum-dried robust bridged silsesquioxane aerogels. *Adv. Mater.* 25, 4494–4497. doi: 10.1002/adma.201301617

Wang, Z., Wang, D., Qian, Z., Guo, J., Dong, H., Zhao, N., et al. (2015). Robust superhydrophobic bridged silsesquioxane aerogels with tunable performances and their applications. *ACS Appl. Mater. Interfaces* 7, 2016–2024. doi: 10.1021/am5077765

Wei, S., Ching, Y. C., and Chuah, C. H. (2020). Synthesis of chitosan aerogels as promising carriers for drug delivery: a review. *Carbohydr. Polym.* 231:115744. doi: 10.1016/j.carbpol.2019.115744

Wei, Y., Wang, J., Zhang, Y., Wang, L., and Zhang, X. (2015). Autocatalytic synthesis of molecular-bridged silica aerogels with excellent absorption and super elasticity. *RSC Adv.* 5, 91407–91413. doi: 10.1039/c5ra19776g

Wong, J., Kaymak, H., Brunner, S., and Koebel, M. M. (2014). Mechanical properties of monolithic silica aerogels made from polyethoxydisiloxanes. *Micropor. Mesopor. Mater.* 183, 23–29. doi: 10.1016/j.micromeso.2013.08.029

Wu, Y., Qiu, H., Sun, J., Wang, Y., Gao, C., and Liu, Y. (2021). A silsesquioxane-based flexible polyimide aerogel with high hydrophobicity and good adsorption for liquid pollutants in wastewater. *J. Mater. Sci.* 56, 3576–3588. doi: 10.1007/s10853-020-05460-2

Yun, S., Luo, H., and Gao, Y. (2014). Ambient-pressure drying synthesis of large resorcinol-formaldehyde-reinforced silica aerogels with enhanced mechanical strength and superhydrophobicity. *J. Mater. Chem. A* 2, 14542–14549. doi: 10.1039/c4ta02195a

Yun, S., Luo, H., and Gao, Y. (2015). Low-density, hydrophobic, highly flexible ambient-pressure-dried monolithic bridged silsesquioxane aerogels. *J. Mater. Chem. A* 3, 3390–3398. doi: 10.1039/c4ta05271d

Zhang, X., Ni, X., Li, C., You, B., and Sun, G. (2020). Co-gel strategy for preparing hierarchically porous silica/polyimide nanocomposite aerogel with thermal insulation and flame retardancy. *J. Mater. Chem. A* 8, 9701–9712. doi: 10.1039/c9ta13011j

Zhang, Y., Wang, J., Wei, Y., and Zhang, X. (2017). Robust urethane-bridged silica aerogels available for water-carved aerosculptures. *New J. Chem.* 41, 1953–1958. doi: 10.1039/c6nj03414d

Ziegler, C., Wolf, A., Liu, W., Herrmann, A., Gaponik, N., and Eychmüller, A. (2017). Modern inorganic aerogels. *Angew. Chem. Int. Ed.* 56, 13200–13221. doi: 10.1002/anie.201611552

Zu, G., Kanamori, K., Maeno, A., Kaji, H., and Nakanishi, K. (2018a). Superflexible multifunctional polyvinylpolydimethylsiloxane-based aerogels as efficient absorbents, thermal superinsulators, and strain sensors. *Angew. Chem. Int. Ed.* 57, 9722–9727. doi: 10.1002/anie.201804559

Zu, G., Kanamori, K., Shimizu, T., Zhu, Y., Maeno, A., Kaji, H., et al. (2018b). Versatile double-cross-linking approach to transparent, machinable, supercompressible, highly bendable aerogel thermal superinsulators. *Chem. Mater.* 30, 2759–2770. doi: 10.1021/acs.chemmater.8b00563

Zu, G., Shimizu, T., Kanamori, K., Zhu, Y., Maeno, A., Kaji, H., et al. (2018c). Transparent, superflexible doubly cross-linked polyvinylpolymethylsiloxane aerogel superinsulators via ambient pressure drying. *ACS Nano* 12, 521–532. doi: 10.1021/acsnano.7b07117

Conflict of Interest: The authors declare that the research was conducted in the absence of any commercial or financial relationships that could be construed as a potential conflict of interest.